

Interface collisions

F. D. A. Aarão Reis¹ and O. Pierre-Louis²

¹ *Instituto de Física, Universidade Federal Fluminense,
Avenida Litorânea s/n, 24210-340 Niterói RJ, Brazil*

² *ILM, University Lyon 1, 43 Bd du 11 novembre 1918, 69622 Villeurbanne, France*

(Dated: February 5, 2019)

Abstract

We provide a theoretical framework to analyze the properties of frontal collisions of two growing interfaces considering different short range interactions between them. Due to their roughness, the collision events spread in time and form rough domain boundaries, which defines collision interfaces in time and space. We show that statistical properties of such interfaces depend on the kinetics of the growing interfaces before collision, but are independent of the details of their interaction and of their fluctuations during the collision. Those properties exhibit dynamic scaling with exponents related to the growth kinetics, but their distributions may be non-universal. These results are supported by simulations of lattice models with irreversible dynamics and local interactions. Relations to first passage processes are discussed and a possible application to grain boundary formation in two-dimensional materials is suggested.

Interface motion and collisions are ubiquitous in non-equilibrium systems. For example, in graphene growth on metal substrates, mono-crystalline domains grow and meet, ultimately forming a polycrystalline film with grain boundaries [1–4]. The formation of rough domain boundaries via interface collisions is encountered in many other systems undergoing domain growth, such as bacterial colonies [7]. Motivated by the selection of grains in crystal growth [8] or of species in population dynamics [9], domain boundary formation has been investigated within competitive growth models, where two interfaces grow in the same direction generating two types of domains growing side by side. The domain boundary exhibits a self-similar behavior [8], which can be affected by the average orientation of the growing interfaces [10]. However, fewer studies have considered domain boundary formation by frontal collisions, where colliding interfaces are parallel in average. Based on simulations of the Eden model, Albano *et al*[11, 12] have exhibited numerical evidence suggesting dynamic scaling.

Furthermore, interface collisions do not always produce a domain boundary, and instead interfaces may simply annihilate. In such cases, the collision spreads in time due to the roughness of the growing fronts. This is for example observed in magnetic domains [13], reaction fronts [14], turbulent liquid crystals [15], burning paper [16], forest fires [17], and layer by layer crystal growth [18].

In this Rapid Communication, we determine both the roughness of the resulting domain boundary, and the spreading of the collision in time during frontal collisions. We use several different models of interface growth with irreversible rules and short range interactions between the two interfaces. We show that the distribution and spatial correlations of collision times and of the resulting domain boundary are independent of the details of the interactions between the two interfaces, and only depend the roughness that builds up before collision. Dynamic scaling appears as a consequence of these results. The asymptotic distributions are dictated by the interface with the largest roughness when the growth exponent of the two colliding interfaces are different, and those distributions are non-universal when the growth exponents are equal.

We performed simulations using well-known one-dimensional irreversible lattice growth models: random deposition (RD) with a sticking coefficient [21], a modified Family model [22], and restricted solid on solid models [23] with maximum height differences 1 (RSOS) or 2 (RSOS2). Their rules are described in Fig. 1(a). The lattice constant is the unit length

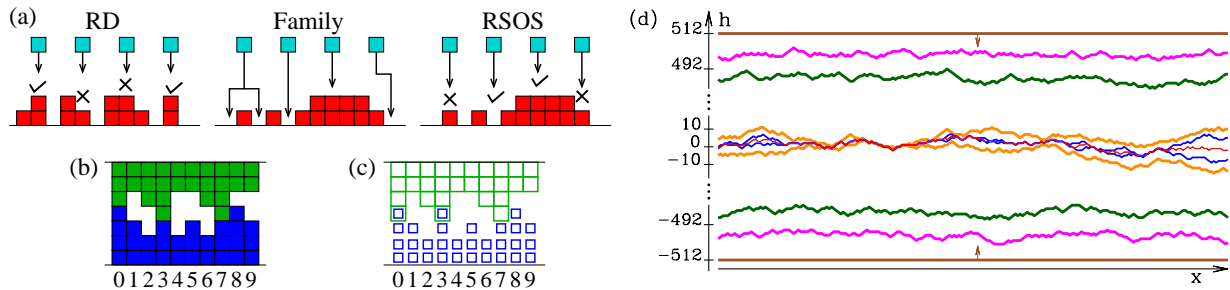


FIG. 1. Interface collision models. (a) Growth models. Random Deposition (RD) model: at each time-step, an incident particle sticks with probability p in each column. Modified Family model: the incident particle aggregates at the column of incidence if no nearest neighbor (NN) column has smaller height; if only one NN has a smaller height, it aggregates at that column, and if two NN columns have smaller heights, one of them is randomly chosen. RSOS models: the particle sticks only if the resulting differences of heights between all NN columns do not exceed 1 (RSOS model) or 2 (RSOS2 model). (b) Schematics of collision with short range interaction, with growth ceasing at columns 0, 3, and 7. (c) Phantom collision, where growth continued in columns 0 (advance of upper interface) and 3 (advance of lower interface). (d) Collision simulation ($d_0 = 2^9$) with two interfaces growing with the RSOS model in opposite directions and colliding with short range interaction.

and the interface length is denoted as L . The unit time is set by L attempts of particle deposition; rejection of such attempts are possible in RSOS and RSOS2 models or after collision events with short range interactions (defined below).

We denote the two interface positions at time t and abscissa x as $h_-(x, t)$ and $h_+(x, t)$. They are initially flat and located at positions $h_{\pm}(x, t = 0) = \pm d_0$. During growth, these interfaces move toward each other and collide. At each x the collision time $t_c(x)$ and the locus of the collision $h_c(x)$ obey

$$h_+(x, t_c(x)) = h_-(x, t_c(x)) = h_c(x). \quad (1)$$

Since we consider irreversible growth models, interfaces only move forward and, consequently, they only pass one time at a given height. Thus, $t_c(x)$ and $h_c(x)$ are uniquely defined by Eq.(1). Collisions are studied when both interfaces are in their growth regimes, i. e. with time increasing roughness [21, 26].

The growth models are supplemented with rules describing the interaction of the interfaces as they collide. The first rule, which is illustrated in Fig. 1(b), accounts in a simple

way for short range interactions: the interfaces stop growing at each column x when they meet, i.e. when Eq.(1) is satisfied. Since particle deposition depends on the height of neighboring sites (except in RD), the collision at a given column affects the subsequent growth of its neighbors. An example of the dynamics with short range interaction is presented in Fig. 1(d). The second rule considers non-interacting interfaces which continue to grow as if the opposite interface was not there. This rule, hereafter denoted as phantom collision, is illustrated in Fig. 1(c) (movies of collisions with both types of rules are reported as Supplemental Material).

We assume that interfaces move with constant and model-dependent average velocities v_{\pm} [24]. We have $v_{\pm} = p_{\pm}$ in RD, and $v = 1$ in the Family model by construction. Moreover, we extracted from simulations $v = 0.41904(10)$ for RSOS, and $v = 0.6036(3)$ for RSOS2. The relative velocity of the two interfaces is $\bar{v} = v_- + v_+$, leading to the average collision time $t_0 = 2d_0/\bar{v}$, while the average position of the collision is $h_0 = d_0(v_- - v_+)/\bar{v}$. The deviations of $t_c(x)$ and $h_c(x)$ from these average values are denoted as

$$\delta t_c(x) = t_c(x) - t_0, \quad (2a)$$

$$\delta h_c(x) = h_c(x) - h_0. \quad (2b)$$

We then define the distributions $F_c(\delta t_c)$ of collision times, and $P_c(\delta h_c)$ of collision loci for an initial distance $2d_0$.

The first striking point revealed by simulations is the irrelevance of short-range interactions on the statistical properties of the collisions. Indeed, for d_0 large enough, the distributions $F_c(\delta t_c)$ and $P_c(\delta h_c)$ in phantom collisions are found to be identical to those with short range interactions. This is shown in Fig. 2 for collision between interfaces governed by identical or different models.

This result suggests that interactions during collision are irrelevant. We thus define the distributions $P_{\pm}(\zeta_{\pm}; t)$ of interface fluctuations $\zeta_{\pm}(x, t) = \mp [h_{\pm}(x, t) - \langle h_{\pm}(x, t) \rangle]$ in absence of collision (with this definition $\zeta > 0$ for fluctuations in the direction of growth). Assuming that interactions are irrelevant, we replace interface fluctuations by ζ_{\pm} , and rewrite Eq. (2) using Eq. (1):

$$\delta t_c(x) = -\frac{\zeta_+(x, t_0 + \delta t_c(x)) + \zeta_-(x, t_0 + \delta t_c(x))}{\bar{v}}, \quad (3a)$$

$$\delta h_c(x) = \frac{-v_- \zeta_+(x, t_0 + \delta t_c(x)) + v_+ \zeta_-(x, t_0 + \delta t_c(x))}{\bar{v}}. \quad (3b)$$

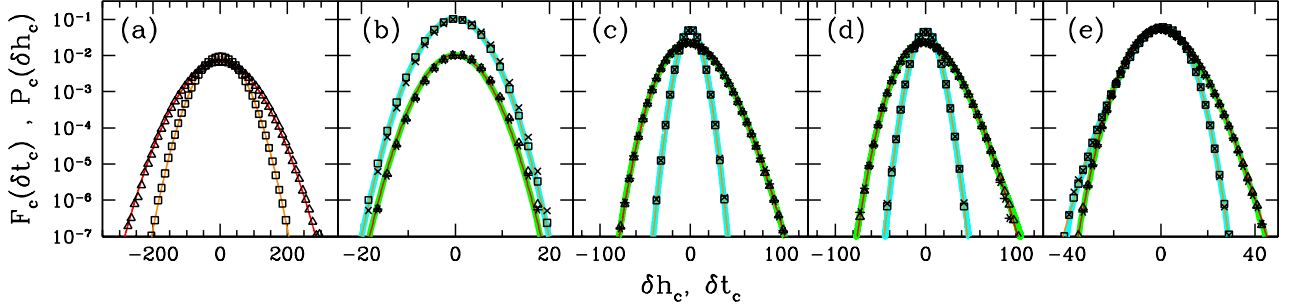


FIG. 2. Distributions of collision times and loci. Models: (a) RD-RD with $p_+ = 0.5$ and $p_- = 1$, (b) Family-Family, (c) RSOS-RSOS, (d) RSOS-RSOS2, (e) RSOS-Family. Symbols indicate simulation results with $d_0 = 2^{12}$ and $L = 2^{32}$, and with short range interaction [\square : $P_c(\delta h_c)$, \triangle : $F_c(\delta t_c)$] or phantom collision [\times : $P_c(\delta h_c)$, $*$: $F_c(\delta t_c)$]. Thick curves are obtained from Eqs. (5a,b) (green, blue) using distributions from interfaces without collision calculated numerically. Thin lines are distributions obtained from Eqs. (5a,b) (red, orange) using theoretical universal distributions (Gaussian or Tracy-Widom) with variances extracted from simulations of interfaces without collisions. In (b), $F_c(\delta t_c)$ is shifted down by one unit for the sake of clarity.

For large t_0 , we expect $\delta t_c(x) \ll t_0$, and hence to leading order we approximate $t_0 + \delta t_c(x)$ by t_0 in the r.h.s. of Eqs.(3). We therefore define

$$\delta t_c^0(x) = -\frac{\zeta_+(x, t_0) + \zeta_-(x, t_0)}{\bar{v}}, \quad (4a)$$

$$\delta h_c^0(x) = \frac{-v_- \zeta_+(x, t_0) + v_+ \zeta_-(x, t_0)}{\bar{v}}. \quad (4b)$$

These quantities can be obtained as follows: (i) perform the evolution as if interfaces could evolve and freely cross without interacting up to time t_0 ; (ii) freeze the interfaces at $t = t_0$ and slide them (forward and backward in time) without shape change and with their own average velocity v_{\pm} ; (iii) measure the collision times $t_c^0(x)$ and locations $h_c^0(x)$. This process, hereafter referred to as the freeze-and-slide approximation, corresponds to a situation where fluctuations during collision are absent.

Since ζ_+ and ζ_- are independent, the probability distributions resulting from Eq.(4) read:

$$F_c(\delta t_c) = \bar{v} \int d\zeta_+ P_+(\zeta_+; t_0) P_-(-\delta t_c \bar{v} - \zeta_+; t_0) \quad (5a)$$

$$P_c(\delta h_c) = \frac{\bar{v}}{v_+} \int d\zeta_+ P_+(\zeta_+; t_0) P_- \left(\frac{-\delta h_c \bar{v} + \zeta_+ v_-}{v_+}; t_0 \right). \quad (5b)$$

Using $P_{\pm}(\zeta_{\pm}, t_0)$ obtained numerically from simulations of interfaces without collision, we calculated these convoluted distributions for collisions with five pairs of models, as shown in Fig. 2. In all cases, there is excellent agreement with distributions obtained in collision simulations, confirming the validity of the freeze-and-slide approximation.

Based on this result, we now show that collision properties obey simple scaling laws. From dynamic scaling [21, 25], time correlation functions of a growing interface are characterized by the growth exponent β :

$$\langle [\zeta(x, t + \tau) - \zeta(x, t)]^2 \rangle = B|\tau|^{2\beta}, \quad (6)$$

as long as the correlation length $\xi_{corr} \sim t^{\beta/\alpha}$ is smaller than the interface length L . The roughness exponent α characterizes spatial correlations at short enough distances $\xi \ll \xi_{corr}$ [21, 26] via

$$\langle [\zeta(x + \xi, t) - \zeta(x, t)]^2 \rangle = A|\xi|^{2\alpha}. \quad (7)$$

Within this description, RD corresponds to diffusive dynamics with $\beta = 1/2$ without lateral correlation. The other models belong to universality classes with subdiffusive time-correlations [21, 26]: Edwards-Wilkinson (EW) class with $\beta = 1/4$ and $\alpha = 1/2$ for the Family model; Kardar-Parisi-Zhang (KPZ) class with $\beta = 1/3$ and $\alpha = 1/2$ for RSOS and RSOS2.

The variances of the distributions $F_c(\delta t_c)$ and $P_c(\delta h_c)$ are obtained from Eq.(4) as

$$\langle \delta t_c(x)^2 \rangle = \frac{B_+ t_0^{2\beta_+} + B_- t_0^{2\beta_-}}{\bar{v}^2}, \quad (8a)$$

$$\langle \delta h_c(x)^2 \rangle = \frac{v_-^2 B_+ t_0^{2\beta_+} + v_+^2 B_- t_0^{2\beta_-}}{\bar{v}^2}. \quad (8b)$$

where we have used that $\langle \zeta_{\pm}(x, t_0)^2 \rangle = B_{\pm} t_0^{2\beta_{\pm}}$ from Eq.(6) with $\zeta_{\pm}(x, t = 0) = 0$. If $\beta_+ = \beta_-$, both terms in the r.h.s. of Eqs.(8) are equally relevant. Otherwise, for $\beta_+ \neq \beta_-$, the term with the largest exponent is asymptotically dominant, and the variances scale with exponent $2\beta_m$, where $m = +$ when $\beta_+ \geq \beta_-$ and $m = -$ when $\beta_- > \beta_+$.

In collisions with the RD model, each column is equivalent to an independent first passage processes, thereby providing an alternative analytical derivation of Eqs.(5,8) in a special case. The resulting distribution for the height h_{\pm} of one column is a binomial distribution [21]. Using Stirling's formula, one obtains a Gaussian distribution for $P(h_{\pm}; t)$ at long times with variance $\langle \zeta_{\pm}^2 \rangle = \langle (h_{\pm} - v_{\pm} t)^2 \rangle = 4D_{\pm} t$, where $v_{\pm} = p_{\pm}$ and $D_{\pm} = p_{\pm}(1 - p_{\pm})/2$ is the

| | | | | |
|--|-----------|-----------|-----------|-----------|
| + | Family | RSOS | RSOS | RSOS |
| - | Family | RSOS | RSOS2 | Family |
| $\beta(\delta t_c)$ | 0.248(5) | 0.329(4) | 0.333(1) | 0.330(15) |
| Eq.(8a) | 1/4 | 1/3 | 1/3 | 1/3 |
| $\langle \delta t_c^2 \rangle / (2d_0)^{2\beta}$ | 0.159(1) | 0.815(2) | 0.761(1) | 0.095(25) |
| Eq.(8a) | 0.1589(4) | 0.814(3) | 0.759(4) | 0.0999(4) |
| $A_{\delta t_c}$ | 0.318(7) | 2.34(2) | 3.6(2) | 0.75(3) |
| Eq.(9a) | 0.320(5) | 2.35(3) | 3.49(7) | 0.728(10) |
| $\beta(\delta h_c)$ | 0.250(2) | 0.333(1) | 0.334(1) | 0.327(3) |
| Eq.(8b) | 1/4 | 1/3 | 1/3 | 1/3 |
| $\langle \delta h_c^2 \rangle / (2d_0)^{2\beta}$ | 0.1593(3) | 0.1435(5) | 0.179(1) | 0.100(5) |
| Eq.(8b) | 0.1589(4) | 0.1429(6) | 0.1785(6) | 0.0999(4) |
| $A_{\delta h_c}$ | 0.320(5) | 0.414(6) | 0.745(15) | 0.475(20) |
| Eq.(9b) | 0.320(5) | 0.413(5) | 0.761(14) | 0.466(5) |

TABLE I. Comparison of exponents and amplitudes calculated in simulations with short range interaction (upper values) and predicted by the freeze-and-slide approximation (lower values).

diffusion constant. Comparison with Eq.(6) leads to $\beta_{\pm} = 1/2$ and $B_{\pm} = 2D_{\pm}$. In one column, the collision then reduces to the first passage process of two particles undergoing biased diffusion toward each other, which has a well known solution [19]. Since columns are independent, the average over realizations leads to the same result as the average over the interface size L , providing the distributions $F_c(\delta t_c)$ and $P_c(\delta h_c)$ (detailed expressions are in the Supplemental Material). In the limit where $d_0 \gg 1$ and $d_0 \gg D_{\pm}/v_{\pm}$, one finds Gaussians in agreement with Eqs.(5), with variances given by Eqs.(8).

For collisions with other models, the estimates of the exponents of the variances of δt_c and δh_c were obtained in simulations and are shown in Table I (numerical procedures are in the Supplemental Material). They agree with the exponent β_m expected from Eq.(8). Using the theoretically predicted value of β_m and the variances from simulations, we calculated the ratios $\langle \delta t_c^2 \rangle / (2d_0)^{2\beta_m}$ and $\langle \delta h_c^2 \rangle / (2d_0)^{2\beta_m}$ and extrapolated them to $d_0 \rightarrow \infty$. As shown in Table I, the results agree with the estimates obtained from Eq.(8) with the values of v and B extracted from simulations of interfaces in the absence of collision [$B = 0.4495(10)$]

for the Family model; $B = 0.254(1)$ for RSOS; $B = 0.552(2)$ for RSOS2].

Beyond exponents, the different universality classes impose that $P(\zeta; t) = f(\zeta/W)/W$, with $W = B^{1/2}t^\beta$ and universal distributions f at long times: Gaussian for RD and EW class, and Tracy-Widom for the KPZ class [27, 28]. Inserting this ansatz into Eq.(5) and using the variances from the corresponding models without collision at t_0 , we obtain distributions F_c and P_c in good agreement with collision simulations, as shown in Fig. 2 (this is confirmed by the analysis of the skewness and kurtosis in the Supplemental Material). If $\beta_+ \neq \beta_-$, this scaling ansatz can be inserted in Eqs.(5). We then find that, to leading order, the distributions of time and locus of collision follow the universal distribution of the growing interface with exponent β_m : $F_c(\delta t_c) = f_m(-\delta t_c/T_c)/T_c$, where $T_c = W_m/\bar{v}$, and $P_c(\delta h_c) = f_m(-\delta t_c/W_c)/W_c$, where $W_c = v_{-m}W_m/\bar{v}$. In contrast, when $\beta_+ = \beta_-$ the distributions P_c and F_c resulting from Eq.(8) cannot be rescaled by a single time or lengthscale; they are non universal in the sense that they depend on (ratios of) non-universal model-dependent parameters (v_\pm and B_\pm).

We now turn to spatial correlations. Approximating δt_c and δh_c by Eq.(4) and using Eq. (7), we find that at distances smaller than the correlation lengths of the two interfaces, spatial correlations obey

$$\langle [\delta t_c(x + \xi) - \delta t_c(x)]^2 \rangle = \frac{A_+ |\xi|^{2\alpha_+} + A_- |\xi|^{2\alpha_-}}{\bar{v}^2}, \quad (9a)$$

$$\langle [\delta h_c(x + \xi) - \delta h_c(x)]^2 \rangle = \frac{v_-^2 A_+ |\xi|^{2\alpha_+} + v_+^2 A_- |\xi|^{2\alpha_-}}{\bar{v}^2}. \quad (9b)$$

Thus, to leading order, correlations scale in ξ with an exponent $\alpha_c = \max[\alpha_+, \alpha_-]$.

In the absence of collisions, the scaling in Eq.(7) is observed numerically in narrow ranges of ξ even at long times. However, using the known values of α_\pm and an extension of the procedure developed in [29], we estimated the amplitudes $A = 0.64(1)$ for the Family model, $A = 0.825(10)$ for RSOS, and $A = 2.82(6)$ for RSOS2. The same method is used to estimate $A_{\delta t_c} \equiv \langle [\delta t_c(x + \xi) - \delta t_c(x)]^2 \rangle / |\xi|^{2\alpha_c}$ and $A_{\delta h_c} \equiv \langle [\delta h_c(x + \xi) - \delta h_c(x)]^2 \rangle / |\xi|^{2\alpha_c}$. The results shown in Table I indicate good agreement between Eq.(9) and the simulations (the convergence to these values is presented in the Supplemental Material). For Family-RSOS collisions, observe that $\alpha_+ = \alpha_-$, thus EW correlations contribute to the lateral correlation of the collision interface at small lengthscales, although distributions F_c and P_c belong to the KPZ class.

In addition, dynamic scaling provides a rationale for the irrelevance of short-range interactions. Indeed, from Eqs.(8), the collision duration $T_c = \langle \delta t_c(x)^2 \rangle^{1/2} \sim W_c/\bar{v}$, where $W_c = \langle \delta h_c(x)^2 \rangle^{1/2}$. Thus, during collision, lateral correlations propagate on a distance $\xi_{coll} \sim T_c^{\beta/\alpha} \sim W_c^{\beta/\alpha}$ (here the indexes of α and β can be + or - without affecting the conclusions). Since the distance between the interfaces during collision is $\sim W_m \sim W_c$, we expect the typical distance between contact points to be $\xi_{contact} \sim W_c^{1/\alpha}$ from Eq.(9b). For normal dynamic scaling, $\beta < \alpha \leq 1$ [21, 26], thus we have $\xi_{coll} \ll W_c \leq \xi_{contact}$ at long times. Hence, interactions influence the collisions in the vicinity of contact points, but these perturbations do not have time to propagate between contact points during the collision time. Thus, interactions are irrelevant to leading order.

Scaling also imposes the irrelevance of fluctuations during collision. Indeed, we have $T_c \sim W_c/\bar{v} \sim t_0^{\beta_m} \ll t_0$, justifying the separation of scales at the origin of the freeze-and-slide approximation. Furthermore, from Eqs. (3,4) and Eq.(6), we have $\langle (\delta t_c - \delta t_c^0)^2 \rangle \sim \langle [\zeta(t_0 + \delta t_c) - \zeta(t_0)]^2 \rangle \sim T_c^{2\beta_m} \sim t_0^{2\beta_m^2}$. Thus, $\langle (\delta t_c - \delta t_c^0)^2 \rangle \ll T_c^2 \sim t_0^{2\beta_m}$. This means that deviations of δt_c from δt_c^0 are negligible, i.e. fluctuations during collision are irrelevant. This result and a similar analysis of $\langle (\delta h_c - \delta h_c^0)^2 \rangle$ are presented in the Supplemental Material. Similarly, when the growing fronts reach the late-times stationary state where the roughness saturates to a value that depends on L, scaling as a function of L is also expected for large L, as observed in simulations in Refs.[11, 12].

As a final remark, we conjecture that our results for irreversible growth should directly extend to growing interfaces with particle attachment and detachment, that may exhibit more than one passage obeying Eq.(1). In such cases, the predictions reported above describe the average passage time for phantom collisions instead of their first passage time. Nevertheless, the difference between the first passage time and the average passage time is dictated by the fluctuations during the collision, which were shown to be irrelevant. As a consequence, the first passage time should also be well approximated by the freeze and slide process and our results should be valid when backward motion of the interfaces is possible. This conclusion is corroborated by the agreement discussed above between the asymptotic behaviors of the irreversible RD model and the continuum biased random walk, which exhibits both forward and backward propagation.

In conclusion, our central result is that local interactions and interface fluctuations during the collision do not affect the asymptotic statistical properties of interface collision. As a

consequence, collision properties exhibit dynamic scaling with universal exponents; however, distributions can be non-universal when $\beta_+ = \beta_-$.

Our results may be investigated with the measurement of grain boundary roughness of two-dimensional materials such as graphene [1–4] and MoS₂ [30, 31]. Assume for example that the radius R of growing two-dimensional grains is proportional to time t , and β is the growth exponent of the two grain edges before collision. From Eq.(8b), we speculate that the roughness of grain boundaries will be $W \sim t^\beta \sim R^\beta$. The relation between W and R should therefore allow one to determine β , providing strong constraints on the possible microscopic growth mechanisms proposed in the literature[32, 33].

As a promising perspective, interface collisions can be considered as a generalization of first passage processes [19, 20], where particles diffuse and stick or annihilate when they meet. As opposed to particles, interfaces present intrinsic roughness, which leads to a spreading of the collision in time (some parts meet earlier than others) and in space (all parts do not meet on the same plane). Hence, advances on first-passage of subdiffusive systems [20, 34] and in exact solutions of kinetic roughening [27, 35, 36] should provide tools to explore the underlying links between interface collisions and first passage processes. Natural ramifications linked to persistence [37], large deviation [38], and extremal statistics[39] of interfaces, also appear when e.g. considering the properties of first and last contacts during interface collisions.

ACKNOWLEDGMENTS

FDAAR acknowledges support by CNPq and FAPERJ (Brazilian agencies) and thanks the hospitality of Université Lyon 1, where part of this work was performed. OPL wishes to thank Nanoheal (EU H2020 research and innovation program under grant agreement No **642976**), and LOTUS (ANR-13-BS04-0004-02 Grant).

-
- [1] L. Gao, J. R. Guest, and N. P. Guisinger, *Nano Letters* **10**, 3512 (2010), pMID: 20677798, <http://dx.doi.org/10.1021/nl1016706>.
- [2] P. Y. Huang, C. S. Ruiz-Vargas, A. M. van der Zande, W. S. Whitney, M. P. Levendorf, J. W.

- Kevek, S. Garg, J. S. Alden, C. J. Hustedt, Y. Zhu, J. Park, P. L. McEuen, and D. A. Muller, *Nature* **469**, 389 (2011).
- [3] Q. Yu, L. A. Jauregui, W. Wu, R. Colby, J. Tian, Z. Su, H. Cao, Z. Liu, D. Pandey, D. Wei, T. F. Chung, P. Peng, N. P. Guisinger, E. A. Stach, J. Bao, S.-S. Pei, and Y. P. Chen, *Nat Mater* **10**, 443 (2011).
- [4] B. Kiraly, E. B. Iski, A. J. Mannix, B. L. Fisher, M. C. Hersam, and N. P. Guisinger, *Nat. Commun.* **4**, 2804 (2013).
- [5] W. J. Evans, L. Hu, and P. Koblinski, *Applied Physics Letters* **96**, 203112 (2010), <http://dx.doi.org/10.1063/1.3435465>.
- [6] S. Merabia and K. Termentzidis, *Phys. Rev. B* **89**, 054309 (2014).
- [7] A. Be'er, H. P. Zhang, E.-L. Florin, S. M. Payne, E. Ben-Jacob, and H. L. Swinney, *Proceedings of the National Academy of Sciences* **106**, 428 (2009), <http://www.pnas.org/content/106/2/428.full.pdf>.
- [8] Y. Saito and H. Müller-Krumbhaar, *Phys. Rev. Lett.* **74**, 4325 (1995).
- [9] J.-T. Kuhr, M. Leisner, and E. Frey, *New Journal of Physics* **13**, 113013 (2011).
- [10] B. Derrida and R. Dickman, *Journal of Physics A: Mathematical and General* **24**, L191 (1991).
- [11] E. V. Albano, *Phys. Rev. E* **56**, 7301 (1997).
- [12] E. V. Albano and I. M. Irurzun, *Journal of Physics A: Mathematical and General* **34**, 9631 (2001).
- [13] L. Krusin-Elbaum, T. Shibauchi, B. Argyle, L. Gignac, and D. Weller, *Nature* **410**, 444 (2001).
- [14] S. Atis, A. K. Dubey, D. Salin, L. Talon, P. Le Doussal, and K. J. Wiese, *Phys. Rev. Lett.* **114**, 234502 (2015).
- [15] K. A. Takeuchi and M. Sano, *Phys. Rev. Lett.* **104**, 230601 (2010).
- [16] J. Maunuksela, M. Myllys, O.-P. Kähkönen, J. Timonen, N. Provatas, M. J. Alava, and T. Ala-Nissila, *Phys. Rev. Lett.* **79**, 1515 (1997).
- [17] N. Guisoni, E. S. Loscar, and E. V. Albano, *Phys. Rev. E* **83**, 011125 (2011).
- [18] A. Pimpinelli and J. Villain, *Physics of Crystal Growth* (Cambridge University Press, 1998).
- [19] S. Redner, *A Guide to First-Passage Processes* (Cambridge University Press, Cambridge, England, 2001).
- [20] R. Metzler, S. Redner, , and G. Oshanin, *First-Passage Phenomena and Their Applications*,

Vol. 35 (World Scientific, Singapor, 2014).

- [21] A. Barabási and H. Stanley, Fractal Concepts in Surface Growth (Cambridge University Press, 1996).
- [22] F. Family, *J. Phys. A: Math. Gen.* **19**, L441 (1986).
- [23] J. M. Kim and J. M. Kosterlitz, *Phys. Rev. Lett.* **62**, 2289 (1989).
- [24] Subdominant terms in the scaling behavior are known to affect front velocities with a slowly varying function [40]. These effects are negligible for the largest d_0 studied here.
- [25] T. Vicsek, Fractal Growth Phenomena (World Scientific, Singapore, 1992).
- [26] J. Krug, *Advances in Physics* **46**, 139 (1997), <http://dx.doi.org/10.1080/00018739700101498>.
- [27] T. Sasamoto and H. Spohn, *Phys. Rev. Lett.* **104**, 230602 (2010).
- [28] C. A. Tracy and H. Widom, *Commun. Math. Phys.* **159**, 151 (1994).
- [29] A. Chame and F. D. A. A. Reis, *Surf. Sci.* **553**, 145 (2004).
- [30] L. Tao, K. Chen, Z. Chen, W. Chen, X. Gui, H. Chen, X. Li, and J.-B. Xu, *ACS Appl. Mater. Interfaces* **9**, 12073 (2017).
- [31] L. Karvonen, A. Saynatjoki, M. J. Huttunen, A. Autere, B. Amirsolaimani, S. Li, R. A. Norwood, N. Pryghambarian, H. Lipsanen, G. Eda, K. Keiu, and Z. Sun, *Nat. Commun.* **8**, 15714 (2017).
- [32] E. Loginova, N. C. Bartelt, P. J. Feibelman, and K. F. McCarty, *New Journal of Physics* **10**, 093026 (2008).
- [33] P. Wu, Y. Zhang, P. Cui, Z. Li, J. Yang, and Z. Zhang, *Phys. Rev. Lett.* **114**, 216102 (2015).
- [34] T. Guérin, N. Levernier, O. Bénichou, and R. Voituriez, *Nature* **534**, 356 (2016).
- [35] P. Calabrese and P. Le Doussal, *Phys. Rev. Lett.* **106**, 250603 (2011).
- [36] J. De Nardis, P. Le Doussal, and K. A. Takeuchi, *Phys. Rev. Lett.* **118**, 125701 (2017).
- [37] A. J. Bray, S. N. Majumdar, and G. Schehr, *Advances in Physics* **62**, 225 (2013), <http://dx.doi.org/10.1080/00018732.2013.803819>.
- [38] B. Meerson, E. Katzav, and A. Vilenkin, *Phys. Rev. Lett.* **116**, 070601 (2016).
- [39] M. Dentz, I. Neuweiler, Y. Méheust, and D. M. Tartakovsky, *Phys. Rev. E* **94**, 052802 (2016).
- [40] S. G. Alves, T. J. Oliveira, and S. C. Ferreira, *J. Stat. Mech.* , P05007 (2013).

Supplemental Material: Interface collisions

F. D. A. Aarão Reis¹ and O. Pierre-Louis²

¹ *Instituto de Física, Universidade Federal Fluminense, Avenida Litorânea s/n, 24210-340 Niterói RJ, Brazil and*

² *ILM, University Lyon 1, 43 Bd du 11 novembre 1918, 69622 Villeurbanne, France*

(Dated: February 5, 2019)

We provide some technical details concerning: (i) the parameters for collision movies; (ii) the distributions of first passage time and locus for two particles undergoing biased diffusion; (iii) the numerical convergence of exponents of the width of the distributions $F_c(\delta t_c)$ and $P_c(\delta h_c)$; (iv) the skewness and kurtosis of these distributions; (v) the numerical convergence of the amplitude of spatial correlations; and (vi) the analysis of the difference between $\delta t_c, \delta h_c$ and $\delta t_c^0, \delta h_c^0$.

I. INTERFACE COLLISION MOVIES

Movie 1 shows collision of RSOS-RSOS interfaces with short range interactions. The system length is $L = 1024$. We used periodic boundaries, and initial half separation $d_0 = 512$. Movie 2 corresponds to the same system in the phantom case. The collision line is in blue.

II. DISTRIBUTIONS OF FIRST PASSAGE TIMES AND LOCI FOR TWO PARTICLES UNDERGOING BIASED DIFFUSION

Here, we obtain the distributions of collision time and collision locus for arbitrary values of d_0 within the continuous time model of biased diffusion. Technical details can be found in Ref. [1].

We define first the independent variables [2]

$$h_\Delta = h_+ - h_-, \quad (1)$$

$$h_\Sigma = \frac{D_- h_+ + D_+ h_-}{D_+ + D_-}. \quad (2)$$

At collision when $h_+ = h_- = h_c$, we have $h_\Delta = 0$ and $h_\Sigma = h_c$. We also define the related constants

$$v_\Delta = -v_+ - v_- = -\bar{v}, \quad (3)$$

$$v_\Sigma = \frac{-v_- D_+ + v_+ D_-}{D_+ + D_-}, \quad (4)$$

$$D_\Delta = D_+ + D_-, \quad (5)$$

$$D_\Sigma = \frac{D_+ D_-}{D_+ + D_-}. \quad (6)$$

The first passage of h_Δ at the origin, providing the distribution of collision times in the RD model, reads [1]

$$F_c(t) = \frac{2d_0}{(4\pi D_\Delta t^3)^{1/2}} e^{-(2d_0 + v_\Delta t)^2 / (4D_\Delta t)}. \quad (7)$$

In the limit $d_0 \gg 1$, this distribution reduces to a Gaussian distribution (with $S = 0$ and $Q = 0$). In this limit, the average collision time and its variance read

$$t_0 = \langle t_c \rangle = \frac{2d_0}{v_+ + v_-}, \quad (8)$$

$$\langle \delta t_c^2 \rangle = \frac{4d_0 (D_+ + D_-)}{(v_+ + v_-)^3}. \quad (9)$$

The distribution of the variable h_Σ is that of a simple biased random walk

$$P_\Sigma(h_\Sigma, t) = \frac{1}{(4\pi D_\Sigma t)^{1/2}} e^{-(\tilde{z} - v_\Sigma t)^2 / (4D_\Sigma t)}, \quad (10)$$

where

$$\tilde{z} = h_\Sigma - d_0 \left(\frac{D_+ - D_-}{D_+ + D_-} \right). \quad (11)$$

Since the variables h_Δ and h_Σ are independent, we obtain the distribution of the locus of collision as

$$P_c(h_c) = \int_0^\infty dt F_c(t) P_\Sigma(h_c, t), \quad (12)$$

leading to

$$P_c(z) = \frac{d_0 \kappa_1}{2\pi D_\Delta^{1/2} D_\Sigma^{1/2} \kappa_2} e^{-d_0 v_\Delta / D_\Delta + \tilde{z} v_\Sigma / (2D_\Sigma)} K_1[\kappa_1 \kappa_2], \quad (13)$$

where K_1 is the modified Bessel function of the second kind and

$$\kappa_1 = \left(\frac{v_\Delta^2}{D_\Delta} + \frac{v_\Sigma^2}{D_\Sigma} \right)^{1/2}, \quad (14)$$

$$\kappa_2 = \left(\frac{d_0^2}{D_\Delta} + \frac{\tilde{z}^2}{D_\Sigma} \right)^{1/2}. \quad (15)$$

Again, in the limit $d_0 \gg 1$, the distribution of the collision locus is Gaussian with $S = 0$ and $Q = 0$. The average and variance read:

$$h_0 = \langle h_c \rangle = \frac{d_0 (v_- - v_+)}{v_+ + v_-}, \quad (16)$$

$$\langle \delta h_c^2 \rangle = \frac{4d_0 (D_+ v_-^2 + D_- v_+^2)}{(v_+ + v_-)^3}. \quad (17)$$

III. CONVERGENCE OF THE EFFECTIVE EXPONENT OF THE WIDTH OF THE DISTRIBUTIONS

Effective exponents were calculated for $\langle \delta t_c^2 \rangle$ with definition

$$\beta^{(eff)}(d_0) \equiv \frac{1}{2} \frac{\ln[\langle \delta t_c^2(d_0) \rangle^{1/2} / \langle \delta t_c^2(d_0/2) \rangle^{1/2}]}{\ln 2}, \quad (18)$$

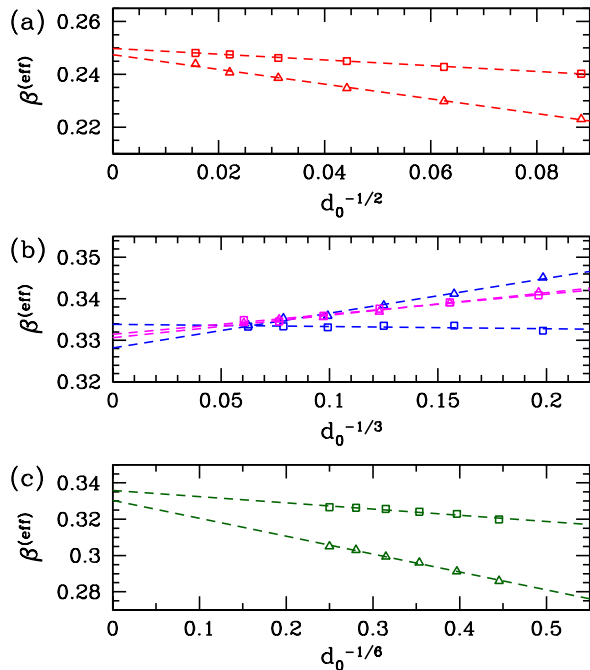


FIG. 1. (Color online) Effective exponents of the variances of the distributions F_c (triangles) and P_c (squares) for collisions with short range interaction: (a) Family-Family; (b) RSOS-RSOS (blue) and RSOS-RSOS2 (magenta); (c) RSOS-Family. Dashed lines are least squares fits of each data set. In (c), the variable in the abscissa accounts for the correction exponent $2\beta_- - 2\beta_+$ suggested by Eqs. (8a) and (8b) of the main text.

and similarly for $\langle \delta h_c^2 \rangle$. Their size-dependence is reported in Fig. 1 for four collision models. The results reported in the first and fourth rows of Table I of the main text are obtained by the extrapolation of those plots to $d_0 \rightarrow \infty$ (linear fits shown in Fig. 1).

IV. SKEWNESS AND KURTOSIS OF THE DISTRIBUTIONS

From Eqs. (4) of the main text, the n th normalized cumulants κ_n read when $\beta_+ = \beta_-$ [3]:

$$\kappa_n(\delta t_c) = (-1)^n \frac{B_+^{n/2} \kappa_n(\zeta_+) + B_-^{n/2} \kappa_n(\zeta_-)}{(B_+ + B_-)^{n/2}}, \quad (19a)$$

$$\kappa_n(\delta h_c) = \frac{(-v_-)^n B_+^{n/2} \kappa_n(\zeta_+) + v_+^n B_-^{n/2} \kappa_n(\zeta_-)}{(v_-^2 B_+ + v_+^2 B_-)^{n/2}} \quad (19b)$$

If $\beta_+ \neq \beta_-$, the roughness of the interface with the smallest β is negligible; in the case $\beta_- > \beta_+$ (rougher lower interface), $(-1)^n \kappa_n(\delta t_c) = \kappa_n(\delta h_c) = \kappa_n(\zeta_m)$; in the case $\beta_- < \beta_+$ (rougher upper interface), $\kappa_n(\delta t_c) = \kappa_n(\delta h_c) = (-1)^n \kappa_n(\zeta_m)$; The resulting predictions for the skewness $S = \kappa_3$ and the kurtosis $Q = \kappa_4$ are shown in Table SSI.

| Collision -/+ | $S(\delta t_c)$ Eq.(19a) | $Q(\delta t_c)$ Eq.(19a) | $S(\delta h_c)$ Eq.(19b) | $Q(\delta h_c)$ Eq.(19b) |
|---------------|-----------------------------|-----------------------------|-----------------------------|-----------------------------|
| Family/Family | 0 -0.005(10) | 0 -0.005(5) | 0 0.001(3) | 0 -0.002(3) |
| RSOS/RSOS | 0.2075... 0.210(5) | 0.0826... 0.084(2) | 0 0.000(1) | 0.0826... 0.082(4) |
| RSOS/RSOS2 | 0.2182(2) 0.218(4) | 0.0939(2) 0.093(5) | 0.007(2) 0.009(2) | 0.08266(3) 0.082(3) |
| RSOS/Family | 0.293... 0.22(3) | 0.165... 0.11(2) | -0.293... -0.295(20) | 0.165... 0.17(2) |

TABLE SI. Skewness S and kurtosis Q of the distributions F_c and P_c of four collision models. The top value is the theoretical estimate based on the distribution of the corresponding universality class (Family: Gaussian, and RSOS and RSOS2: Tracy-Widom with[4, 5] $S \approx 0.2935$ and $Q \approx 0.1652$).

The simulation values of S and Q are also shown in Table SSI. The results for Family-Family, RSOS-RSOS, and RSOS-RSOS2 collisions are in good agreement with the theoretical prediction.

In the case of RSOS-Family model, good agreement is also observed for collision locus. However, discrepancies are observed in the results in Table SSI for the collision times. Note that the RSOS-Family case, where one interface (Family) should be asymptotically irrelevant as compared to the other (RSOS), is different from the other cases that we have considered, where both interfaces are relevant. As a consequence in the RSOS-Family case, we have to reach large enough d_0 (or t_0) for the Family contribution to become small. Comparing the contributions of both interfaces to the variance, for $d_0 = 4096$ (the largest initial distance considered here), we find $\langle \zeta_+^2(t_0) \rangle / \langle \zeta_-^2(t_0) \rangle \approx (B_+/B_-) t_0^{2(\beta_+ - \beta_-)} \sim 0.44$; for $d_0 = 128$ (smallest distance), this ratio is ~ 0.79 . These corrections affect the estimates of effective exponents; in Fig. (1c), the value for $d_0 = 128$ is closer to the EW value (0.25) than the KPZ value (1/3). Despite this poor separation of scales, the extrapolation in Fig. (1c) still permitted to overcome these deviations and to obtain a value of the exponent in agreement with the predictions, both for δt_c and δh_c . However, an inspection of Fig.(1c) reveals that the convergence of the properties of δh_c are faster than the convergence of the properties of δt_c . This convergence is actually improved by the presence of a factor $(v_+/v_-)^2$ that decreases the subdominant contribution to the variance of δh_c . In the absence of such factor, higher order moments of δt_c could not be obtained with a good accuracy.

V. CONVERGENCE OF THE AMPLITUDE OF SPATIAL CORRELATIONS

For most values of d_0 considered here, the log-log plots of $\langle (\delta h_c(x + \xi) - \delta h_c(x))^2 \rangle$ and $\langle (\delta t_c(x + \xi) - \delta t_c(x))^2 \rangle$ versus $|\xi|$ do not fit a straight line for small values of $|\xi|$, even in narrow ranges of this variable. This paral-

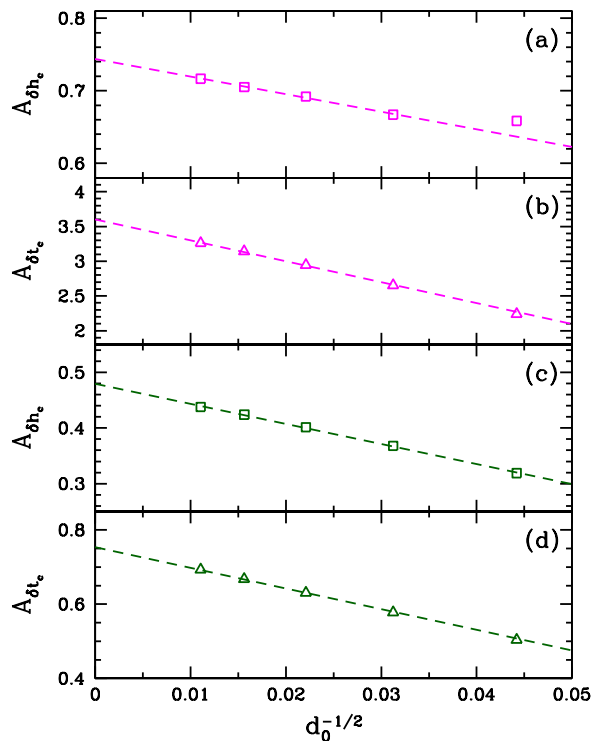


FIG. 2. (color online) Amplitudes of the spatial correlation functions of the collision times (triangles) and of the collision positions (squares) in (a),(b) RSOS-RSOS2 collisions and (c),(d) RSOS-Family collisions. The variable in the abscissa provides the best linear fits of the last 4 or 5 data points in each model.

lels the observations in [6] for the local roughness scaling. For this reason, an extrapolation approach was used along the same lines of that work. First, the ratios $A_{\delta h_c}(d_0) \equiv \langle (\delta h_c(x+\xi) - \delta h_c(x))^2 \rangle / |\xi|^{2\alpha_c}$ and $A_{\delta t_c}(d_0) \equiv \langle (\delta t_c(x+\xi) - \delta t_c(x))^2 \rangle / |\xi|^{2\alpha_c}$ were calculated for three or four fixed values of ξ with the expected exact exponent α_c ; the values of ξ used here were between 8 and 64, so that they are not very small but also do not exceed the lateral correlation length ξ_{corr} , which indicates the saturation of those ratios. Subsequently, those ratios were plotted as a function of $d_0^{-1/2}$ for each value of ξ ; the linear fits of those plots converge to approximately the same values in the limit $d_0 \rightarrow \infty$; this confirms the scaling $\langle (\delta h_c(x+\xi) - \delta h_c(x))^2 \rangle \sim A_{\delta h_c} |\xi|^{2\alpha_c}$ for very large d_0 (and equivalent for δt_c). Fig. 2 illustrates the extrapolation of data with $\xi = 16$ for RSOS-RSOS2 and RSOS-Family collisions. The asymptotic estimates for these and for the other collision models are presented in Table I of the main text. They agree with the predictions from Eqs. (9) of the main text. Note that both terms in Eqs. (9a) and (9b) contribute to the amplitudes of RSOS-Family collisions because both interface models have the same exponent $\alpha = 1/2$.

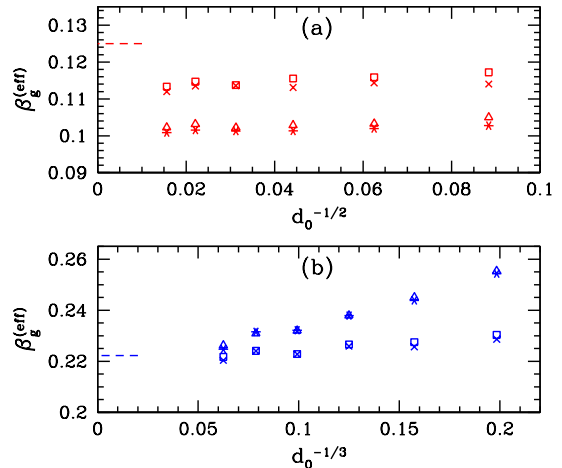


FIG. 3. (Color online) Effective exponents of the correlation functions for (a) Family-Family and (b) RSOS-RSOS collisions with short range interaction: squares $G_{\delta h_c}$, $\phi = 1/1024$; crosses $G_{\delta h_c}$, $\phi = 1/512$; triangles $G_{\delta t_c}$, $\phi = 1/1024$; asterisks $G_{\delta t_c}$, $\phi = 1/512$. Dashed lines indicate the theoretically predicted exponents. The variables in the abscissas were chosen to provide the best linear fits (not shown) in the range of d_0 considered here.

VI. DIFFERENCE BETWEEN δh_c^0 , δt_c^0 , AND δt_c , δh_c

The difference between freeze-and-slide collisions and collisions observed in simulation informs us about the influence of fluctuations during the collision, and is quantified by the correlation functions

$$G_{\delta t_c} = \langle [\delta t_c(x) - \delta t_c^0(x)]^2 \rangle, \quad (20a)$$

$$G_{\delta h_c} = \langle [\delta h_c(x) - \delta h_c^0(x)]^2 \rangle. \quad (20b)$$

As discussed in the main text, we expect

$$G_{\delta t_c} \sim t_0^{\beta_g}, \quad \beta_g = 2\beta_m^2. \quad (21)$$

A similar reasoning also indicates that $G_{\delta h_c} \sim t_0^{\beta_g} \ll \langle \delta h_c^0(x)^2 \rangle$, and $\langle \delta h_c(x)^2 \rangle \approx \langle \delta h_c^0(x)^2 \rangle$.

In simulations with short range interactions, we considered a definition of a time $t_0(\phi)$ at which a fraction ϕ of the sites have collided. The values of ϕ are small, so that the largest part of the interface was not affected by the collision at that time. For a given ϕ , effective exponents of $G_{\delta t_c}$ and $G_{\delta h_c}$ are defined similarly to Eq.(18). In Fig. 3, we show those effective exponents for Family-Family and RSOS-RSOS collisions considering two values of ϕ . The estimates of β_g for large d_0 (large t_0) are close to the values predicted by Eq. (21), which supports the claim that the interface morphology exhibits negligible changes during collision [deviations to smaller β_g for Family-Family collisions in Fig. 3 do not invalidate this reasoning]. Also note that the precise definition of t_0 (related to the value of ϕ in Fig. 3) does not affect the

scalings as long as the reference time t_0 is located during the collision.

- [1] S. Redner, A Guide to First-Passage Processes (Cambridge University Press, Cambridge, England, 2001).
- [2] E. Lucas and E. King, *Ann. Math. Statist.* **25**, 389 (1954).
- [3] If μ_n is the n -th order cumulant, then $\kappa_n = \mu_n / \mu_2^{n/2}$.
- [4] T. Sasamoto and H. Spohn, *Phys. Rev. Lett.* **104**, 230602 (2010).
- [5] P. Calabrese and P. Le Doussal, *Phys. Rev. Lett.* **106**, 250603 (2011).
- [6] A. Chame and F. D. A. A. Reis, *Surf. Sci.* **553**, 145 (2004).